

See discussions, stats, and author profiles for this publication at: <https://www.researchgate.net/publication/8551176>

Structure and Dynamics of a Dihydrogen/Hydride Ansa Molybdenocene Complex

ARTICLE *in* INORGANIC CHEMISTRY · JUNE 2004

Impact Factor: 4.76 · DOI: 10.1021/ic0496875 · Source: PubMed

CITATIONS

33

READS

35

6 AUTHORS, INCLUDING:



Vincent Pons

Laurent & Charras, Lyon, France

18 PUBLICATIONS 1,352 CITATIONS

SEE PROFILE



Stephen L J Conway

University of Oxford

7 PUBLICATIONS 110 CITATIONS

SEE PROFILE



Jennifer C Green

University of Oxford

393 PUBLICATIONS 8,758 CITATIONS

SEE PROFILE

Structure and Dynamics of a Dihydrogen/Hydride Ansa Molybdenocene Complex

Vincent Pons,[†] Stephen L. J. Conway,[†] Malcolm L. H. Green,[†] Jennifer C. Green,[†] Benjamin J. Herbert,[†] and D. Michael Heinekey^{*,†}*Department of Chemistry, University of Washington, Box 351700, Seattle, Washington 98195-1700, and Inorganic Chemistry Laboratory, University of Oxford, South Parks Road, Oxford, OX1 3QR, U.K.*

Received March 10, 2004

In contrast to $[\text{Cp}_2\text{MoH}_3]^+$, which is a thermally stable trihydride complex, the ansa-bridged analogue $[(\eta\text{-C}_5\text{H}_4)_2\text{-CMe}_2\text{MoH}(\text{H}_2)]^+$ (**1**) is a thermally labile dihydrogen/hydride complex. Partial deuteration of the hydride ligands allows observation of $J_{\text{H-D}} = 11.9$ Hz in **1-d**₁ and 9.9 Hz in **1-d**₂ (245 K), indicative of a dihydrogen/hydride structure. There is a slight preference for deuterium to concentrate in the dihydrogen ligand. A rapid dynamic process interchanges the hydride and dihydrogen moieties in complex **1**. Low temperature ¹H NMR spectra of **1** give a single hydride resonance, which broadens at very low temperature due to rapid dipole–dipole relaxation ($T_1 = 23$ ms (750 MHz, 175 K) for the hydride resonance in **1**). Low temperature ¹H NMR spectra of **1-d**₂ allow the observation of decoalescence at 180 K into two resonances. The bound dihydrogen ligand exhibits hindered rotation with $\Delta G^\ddagger_{150} = 7.4$ kcal/mol, but H atom exchange is still rapid at all accessible temperatures (down to 130 K). Density functional calculations confirm the dihydrogen/hydride structure as the ground state for the molecule and give estimates for the energy of two hydrogen exchange processes in good agreement with experiment. The presence of the C ansa bridge is shown to decrease the ability of the metallocene fragment to donate to the hydrogens, thus stabilizing the $(\eta^2\text{-H}_2)$ unit and modulating the barrier to H₂ rotation.

Since the report of the first transition metal dihydrogen complexes,¹ the possibility that a fluxional polyhydride complex might also contain a dihydrogen ligand has been actively investigated.² In this context, the dynamic behavior of prototypical complexes containing one dihydrogen and one hydride ligand is of particular interest. Excluding the large group of known complexes with hydride and dihydrogen ligands trans to each other, which exhibit relatively high barriers to site exchange between hydride and dihydrogen ligands,³ we have focused on complexes with hydride and dihydrogen ligands in cis positions. Several complexes of

this type have been reported. All show interesting dynamic properties, exhibiting rapid exchange of hydrogen environments between the dihydrogen and the hydride ligands, as revealed by variable temperature NMR studies. Early examples of this situation include the iridium complex $[\text{IrH}(\text{H}_2)(\text{bq})(\text{PPh}_3)_2]^+$ (bq = benzoquinolate), which was reported by Crabtree and co-workers to undergo hydrogen atom exchange between the dihydrogen and hydride ligands with $\Delta G^\ddagger_{240} = 10$ kcal/mol.⁴ An iron complex $[\text{FeP}(\text{CH}_2\text{CH}_2\text{CH}_2\text{-PMe}_2)_3(\text{H}_2)\text{H}]^+$, which has $\Delta G^\ddagger_{200} = 9.1$ kcal/mol for permutation of the hydrogen environments, was reported by Field and Bampos.⁵ In these and most other reported examples⁶ of cis dihydrogen/hydride complexes, atom exchange between the hydride and dihydrogen environments

* Author to whom correspondence should be addressed. E-mail: heinekey@chem.washington.edu.

[†] University of Washington.

[‡] University of Oxford.

- (1) Kubas, G. J.; Ryan, R. R.; Swanson, B. I.; Vergamini, P. J.; Wasserman, H. J. *J. Am. Chem. Soc.* **1984**, *106*, 451. General review: Kubas, G. J. *Metal Dihydrogen and σ Bond Complexes*; Kluwer Academic/Plenum Publishers: New York, 2001. Review of computational studies: Maseras, F.; Lledós, A.; Clot, E.; Eisenstein, O. *Chem. Rev.* **2000**, *100*, 601.
- (2) Cf.: Gusev, D. G.; Kuhlman, R. L.; Renkema, K. B.; Eisenstein, O.; Caulton, K. G. *Inorg. Chem.* **1996**, *35*, 6775 and references therein.
- (3) Jessop, P. G.; Morris, R. H. *Coord. Chem. Rev.* **1992**, *121*, 155.

- (4) Crabtree, R. H.; Lavin, M.; Bonnevot, L. *J. Am. Chem. Soc.* **1986**, *108*, 4032.

- (5) Bampos, N.; Field, L. D. *Inorg. Chem.* **1990**, *29*, 587.

- (6) Other reported cis dihydrogen/hydride complexes: Bianchini, C.; Peruzzini, M.; Zanolini, F. *J. Organomet. Chem.* **1988**, *354*, C19. Jia, G.; Drouin, S. D.; Jessop, P. G.; Lough, A. J.; Morris, R. H. *Organometallics* **1993**, *12*, 906. Bianchini, C.; Perez, P. J.; Peruzzini, M.; Zanolini, F.; Vacca, A. *Inorg. Chem.* **1991**, *30*, 279. See also ref 3, page 200.

also requires significant rearrangement on the part of the ancillary ligands, which might be expected to contribute substantially to the activation energy for the process.

Highly symmetric cis dihydrogen/hydride complexes in which no heavy atom rearrangement is required to effect hydrogen atom exchange are much less studied. Iridium dihydrogen/hydride complexes of the form $[\text{TpIr}(\text{PR}_3)(\text{H}_2)\text{H}]^+$ ^{7,8} exhibit a rapid dynamic process which exchanges the hydride and dihydrogen environments. Unfortunately, this process is sufficiently rapid that no low temperature limiting ^1H NMR spectrum could be obtained. The barrier to the site exchange process was estimated to be less than 4.5 kcal/mol.⁷ Ru complexes such as $[(\text{PCy}_3)_2\text{Ru}(\text{CO})_2(\text{H}_2)\text{H}]^+$ exhibit very rapid hydride/dihydrogen exchange, with a barrier measured by very low temperature NMR spectroscopy of $\Delta G^\ddagger_{128} = 5.5$ kcal/mol.⁹ The extremely facile reversible cleavage of a relatively strong H–H bond in these complexes is remarkable and suggests a highly concerted reaction in which a substantial degree of bond formation accompanies the cleavage reaction.

Metallocene complexes have been used to prepare some very important examples of early metal dihydrogen complexes. Of particular interest are species such as $[\text{Cp}_2\text{Ta}(\text{CO})(\text{H}_2)]^+$, which have a d^2 configuration, leading to significant barriers to rotation of bound dihydrogen.¹⁰ Related trihydrides such as $[\text{Cp}_2\text{MH}_3]^+$ ($\text{M} = \text{Mo}, \text{W}$) were reported by Wilkinson and co-workers very early in the development of metallocene chemistry.¹¹ While the tungsten trihydride has a static structure, the Mo analogue is highly fluxional and exhibits quantum mechanical exchange coupling in low temperature ^1H NMR spectra.¹² More recent work by Green and co-workers has demonstrated that the incorporation of ansa bridges can significantly modify the dynamic properties of these molecules. For example, ansa tungstenocene species such as $[(\eta\text{-C}_5\text{H}_4)_2\text{CMe}_2\text{WH}_3]^+$ show very rapid hydride atom exchange at ambient temperature. Low temperature NMR spectroscopy reveals extremely large exchange couplings.¹³

We now report our studies of an ansa molybdenocene complex $[(\eta\text{-C}_5\text{H}_4)_2\text{CMe}_2\text{MoH}(\text{H}_2)]^+$ (**1**), which is a thermally labile dihydrogen/hydride complex, in contrast to the unsubstituted Cp complex $[\text{Cp}_2\text{MoH}_3]^+$, which is a stable trihydride species. The presence of the ansa bridge apparently favors the formation of a bound dihydrogen ligand, which does not undergo formal oxidative addition to afford a Mo^{VI} trihydride as observed in the absence of the ansa bridge.

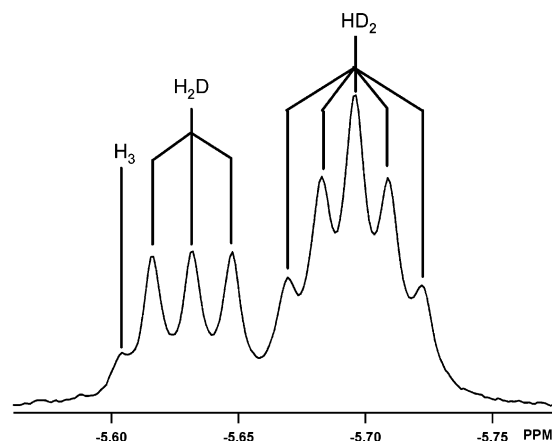


Figure 1. Partial (hydride region) ^1H NMR spectrum of complex **1** at 245 K (750 MHz) with D incorporated in the hydride ligands. $J_{\text{H-D}}$ values are 11.9 Hz for **1-d**₁ and 9.9 Hz for **1-d**₂.

Density functional theory (DFT) calculations verify that the dihydrogen/hydride structure is preferred to the trihydride structure when an ansa bridge is present. Complex **1** is one of a small number of reported H_2 complexes with a d^2 configuration at the metal center and is the first example of a cis dihydrogen/hydride complex with this electronic configuration. Complex **1** exhibits novel dynamic behavior in which hindered dihydrogen rotation can be studied by low temperature NMR spectroscopy. DFT calculations of the barrier to rotation are consistent with the experimental observations.

Results

Synthesis and Characterization of 1. Protonation of the neutral ansa dihydride $(\eta\text{-C}_5\text{H}_4)_2\text{CMe}_2\text{MoH}_2$ with $\text{H}(\text{OEt}_2)_2\text{-(BARF}_4)$ ($\text{ArF} = 3,5\text{-C}_6\text{H}_3(\text{CF}_3)_2$) affords a cationic species **1** which is thermally labile above 260 K. Low temperature ^1H NMR spectra (250 K) of complex **1** reveal a single new hydride resonance at $\delta = -5.59$ ppm (3H) in addition to appropriate resonances for the Cp ring protons and the methyl groups of the ansa bridge. At lower observation temperatures, considerable line broadening of the hydride resonance was observed. Relaxation time determinations revealed a T_1 of 23 ms at 175 K (750 MHz) for the hydride resonance. The maximum rate of relaxation (min T_1) could not be reached, but this value is indicative of the presence of a dihydrogen ligand (see Discussion).

Complex **1** decomposes with loss of H_2 over the course of several hours at temperatures ≥ 260 K. The rate of decomposition was not significantly affected by the presence of an atmosphere of H_2 . Attempts to incorporate deuterium in the hydride sites of **1** by exposure of solutions to D_2 gas at low temperature were not successful.

Complex **1** was prepared in a partially deuterated form by reaction of $(\eta\text{-C}_5\text{H}_4)_2\text{CMe}_2\text{MoH}_2$ with $(\text{CF}_3\text{SO}_2)_2\text{CD}_2$. The hydride region ^1H NMR spectrum at 245 K of a typical partially deuterated sample is shown in Figure 1. The signal due to **1-d**₁ is a 1:1:1 triplet with $J_{\text{H-D}} = 11.9$ Hz while the resonance attributed to **1-d**₂ gives the expected five line pattern with $J_{\text{H-D}} = 9.9$ Hz. The signal due to **1-d**₁ is shifted

- (7) Oldham, W. J., Jr.; Hinkle, A. S.; Heinekey, D. M. *J. Am. Chem. Soc.* **1997**, *119*, 11028.
- (8) Heinekey, D. M.; Oldham, W. J., Jr. *J. Am. Chem. Soc.* **1994**, *116*, 3137.
- (9) Heinekey, D. M.; Mellows, H.; Pratum, T. *J. Am. Chem. Soc.* **2000**, *122*, 6498.
- (10) Sabo-Etienne, S.; Rodriguez, V.; Donnadiou, B.; Chaudret, B.; El Makarim, H. A.; Barthelat, J. C.; Ulrich, P.; Limbach, H. H.; Moïse, C. *New J. Chem.* **2001**, *25*, 55.
- (11) Green, M. L. H.; McLeverty, J. A.; Pratt, L.; Wilkinson, G. *J. Chem. Soc.* **1961**, 4854.
- (12) Heinekey, D. M. *J. Am. Chem. Soc.* **1991**, *113*, 6074.
- (13) Chernega, A.; Cook, J.; Green, M. L. H.; Labella, L.; Simpson, S. J.; Souter, J.; Stephens, A. H. *J. Chem. Soc., Dalton Trans.* **1997**, 3225.

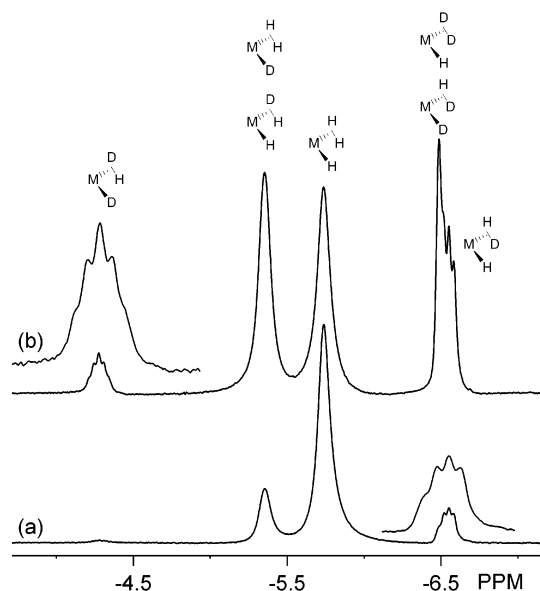


Figure 2. Partial (hydride region) ^1H NMR spectrum of complex **1**, **1-d**₁, and **1-d**₂ at 145 K (500 MHz): (a) low level of deuteration; (b) high level of deuteration.

upfield from **1** by $\Delta\delta = 30$ ppb, while the signal due to **1-d**₂ is upfield by $\Delta\delta = 80$ ppb. The H–D coupling constants show slight temperature dependence, consistent with the operation of isotopic perturbation arising from nonstatistical deuterium distribution. These observations, taken together with the T_1 data, suggest formulation of complex **1** as a dihydrogen/hydride complex $[(\eta\text{-C}_5\text{H}_4)_2\text{CMe}_2\text{MoH}(\text{H}_2)]^+$ (see Discussion).

Highly deuterated samples of **1** were prepared by reaction of $(\eta\text{-C}_5\text{H}_4)_2\text{CMe}_2\text{MoH}_2$ with excess $(\text{CF}_3\text{SO}_2)_2\text{CD}_2$ at 200 K in methylene chloride or Freon solutions. The resulting samples contained predominantly **1-d**₂, with smaller amounts of **1-d**₁ and some **1**. Low temperature ^1H NMR spectra were recorded in $\text{CDF}_2\text{Cl}/\text{CDF}_3$ mixtures. Typical spectra of the hydride region at low temperature are shown in Figure 2. A collection of spectra at a variety of temperatures can be found in the Supporting Information. The assignments of resonances to the various isotopomers is based on the examination of several samples with varying levels of deuteration.

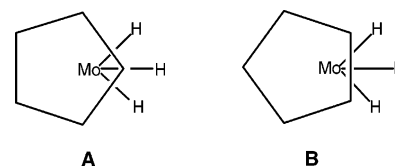
For **1-d**₂, decoalescence to give two hydride signals is observed at ca. 180 K. The signal at -4.25 ppm corresponds to one hydride and is broad, while the signal at -6.50 ppm corresponds to two hydrides and is somewhat sharper. Further cooling allows the resolution of a five line pattern in the resonance at -4.28 ppm, with $J_{\text{H-D}} = 15.6$ Hz. No H–D coupling is resolvable in the resonance at -6.49 ppm. The signal due to **1** is a single resonance at all accessible temperatures, while **1-d**₁ gives two distinct resonances at -5.35 ppm and -6.55 ppm. Interpretation of the low temperature spectra of the various isotopomers is detailed in the Discussion section.

Computational Results. Density functional theory was used to model the related set of compounds **1**, $[(\eta\text{-C}_5\text{H}_4)_2\text{-SiMe}_2\text{MoH}_3]^+$ (**2**), and $[\text{Cp}_2\text{MoH}_3]^+$ (**3**). Energies quoted are for differences in stationary points on the energy surface, except where otherwise specified. Geometry optimizations,

Table 1. Selected Structural Parameters for the Ground State Structures of **1**, **2**, and **3**

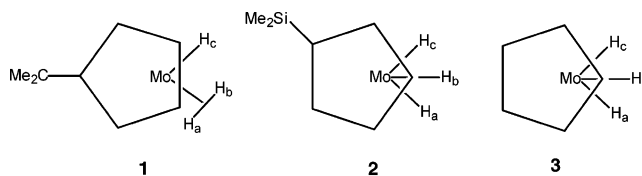
	1	2	3
Mo–H _a	1.768	1.682	1.667
Mo–H _b	1.782	1.695	1.680
Mo–H _c	1.688	1.669	1.667
H _a –H _b	0.985	1.660	1.648
H _b –H _c	1.832	1.606	1.649
Mo–C _{av}	2.276	2.288	2.294
Mo–C _{pcent}	1.927	1.942	1.951
C–C _{av}	1.423	1.424	1.418
α	60	45	29
C _{pcent} –Mo–C _{pcent}	128	138	151
β	162	155	

with no symmetry restrictions, were used to find the ground state structure in each case. The lowest energy structure for **1** was found to be $[(\eta\text{-C}_5\text{H}_4)_2\text{CMe}_2\text{MoH}(\eta^2\text{-H}_2)]^+$ with a bound dihydrogen ligand. Compound **3** has a trihydride ground state of C_{2v} symmetry. The orientation of the cyclopentadienyl rings is such that four carbons occupy the back of the metallocene wedge (**A**); the alternative C_{2v} structure (**B**) with two carbons at the back of the wedge was calculated to be 7.6 kcal/mol higher in energy.



The Si ansa bridged species **2** has a trihydride ground state, which is distorted from C_{2v} symmetry to form a structure analogous to **A** with four carbons at the back. The Si sits to one side of the vector defined by Mo and the central hydrogen atom, H_b. Attempts to optimize a $(\text{H}_2)\text{H}$ structure for $[(\eta\text{-C}_5\text{H}_4)_2\text{SiH}_2\text{MoH}_3]^+$ gave a structure 1.3 kcal/mol higher in energy but with two imaginary frequencies, one at $-213i$ corresponding to H–H stretch, and one at $-80i$ corresponding to ring motion. Calculations by others using different functionals and basis sets come to an opposite conclusion for Si bridged species, in that they find a $(\text{H}_2)\text{H}$ structure to be the ground state; our methodology gives them as very close in energy.¹⁴

Table 1 gives selected calculated structural parameters for **1**, **2**, and **3** (α is the angle between the ring planes; β is the angle between the bridging atom–*ipso*-carbon vector and the *ipso*-carbon ring centroid vector; H_a and H_b form the rotating H₂ unit).



H atom exchange processes were investigated by linear transits and optimizing transition states. For all three molecules, interchange of H_a and H_b was preceded by rotation of H_a–H_b out of the metallocene plane and a transition state

(14) Parkin, G. Personal communication.

Table 2. Selected Structural Parameters for the C_{2v} Transition States

	1	2
Mo–H _a	1.687	1.676
Mo–H _b	1.711	1.699
H _a –H _b	1.523	1.557
Mo–C _{av}	2.270	2.298
Mo–C _{pcent}	1.941	1.954
C–C _{av}	1.422	1.422
α	59	46
C _{pcent} –Mo–C _{pcent}	128	139
β	161	157

Table 3. Selected Structural Parameters for the C_s Transition States

	1	2	3
Mo–H _a	1.910	1.887	1.867
Mo–H _c	1.694	1.684	1.676
H _a –H _c	0.828	0.836	0.842
Mo–C _{av}	2.261	2.255	2.276
Mo–C _{pcent}	1.908	1.922	1.928
C–C _{av}	1.427	1.427	1.422
α	61	48	38
C _{pcent} –Mo–C _{pcent}	129	139	147
β	163	159	

with C_s symmetry was found with the unit perpendicular to the plane. The activation energies for H₂ rotation are 10.9, 13.7, and 21.6 kcal/mol for **1**, **2**, and **3** respectively, showing the effect of the ansa bridge in reducing the barrier to rotation. For **2** and **3** the rings rotate in the transition state to conformation **B**. For **1** and **2** the exchange of H_a and H_c was also investigated. For **1** the transition state for this process is of C_{2v} symmetry and is 2.4 kcal/mol higher in energy than the dihydrogen/hydride ground state. For **2**, the exchange of H_a and H_c also proceeded via a C_{2v} structure with the Si atom on the C_2 axis passing through Mo and H_b. The transition state lay 0.9 kcal/mol above the ground state. Dimensions for the transition states are given in Tables 2 and 3.

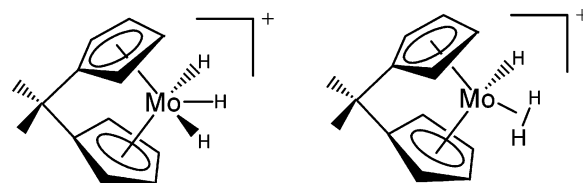
Discussion

Preparation of Complex 1. Complex **1** is readily prepared by protonation of the neutral dihydride precursor with a variety of acids (HBArF₄, trifluoroacetic acid, CH₂(SO₂-CF₃)₂). Isolation of complex **1** is not possible, due to rapid loss of H₂ at temperatures of 270 K and above. A complex mixture of decomposition products is observed, even in Freon solvents. No enhancement of thermal stability is observed under an atmosphere of hydrogen, suggesting that a highly reactive 16 electron species is formed by hydrogen loss, which then quickly reacts with solvent or counteranion. Consistent with these observations, attempts to incorporate deuterium into the hydride positions in **1** by treatment with D₂ gas were not successful. Ultimately, deuterium was incorporated by treatment of solutions of **1** with (CF₃SO₂)₂-CD₂. The degree of deuterium incorporation was varied by varying the ratio of acid to neutral dihydride.

The instability of **1** with respect to loss of H₂ is in contrast to the enhancement of thermal stability reported for neutral ansa Mo^{IV} and W^{IV} complexes. It has been established that this stabilization arises from the inability of the metallocene fragment resulting from reductive elimination to achieve a

structure with parallel rings.¹⁵ In contrast, ansa Ta^V trihydride complexes have been shown to exhibit enhanced rates of H₂ loss in comparison to their nonbridged analogues.¹⁶

Structure of Complex 1. The nonbridged Cp analogue of complex **1** is a trihydride complex, with interesting dynamic behavior featuring significant exchange coupling.¹² Facile loss of H₂ from **1** is suggestive of a dihydrogen/hydride structure. Two possible structures are depicted below.



In principle, these two structures can be distinguished by measurement of relaxation rates for the hydride ligands. The measurement of T_1 values for the hydride resonance in complex **1** was performed at temperatures between 240 and 170 K using a 750 MHz instrument. The measured T_1 decreases to a value of 23 ms at 182 K. Although a true minimum could not be attained, this value is a reasonable estimate for $T_{1(\text{min})}$. This short T_1 value observed for the hydride ligands in complex **1** is qualitatively consistent with the presence of a bound dihydrogen ligand in a hydride/dihydrogen structure. The H–H bond length can be estimated from the mutual dipole–dipole relaxation rate R_{d-d} of the ¹H nuclei in the H₂ ligand ($R_{d-d} = 1/T_{1(d-d)}$). The total relaxation rate R_{H_2} is the sum of R_{d-d} and other relaxation rates from interaction with other magnetic dipoles in the complex, R_o ($R_{H_2} = R_{d-d} + R_o$). In the case of **1**, the R_{obs} value is the weighted average of the relaxation rates of a ¹H atom in all sites. Thus, $R_{\text{obs}}(\mathbf{1}) = (2R_{H_2} + R_H)/3$ where R_{H_2} and R_H are relaxation rates of the H₂ and terminal hydride ligands, respectively. We assume that R_H is modeled by the relaxation rate $R_{\text{obs}}(\text{MoH}_2)$ of the hydride ligand in the neutral dihydride complex ($T_{1(\text{min})}$ of MoH₂ = 1.01 s, 195 K, 750 MHz) and, further, that this rate also approximates R_o . Therefore, as previously derived,⁷

$$R_{\text{obs}}(\mathbf{1}) = (2R_{H_2} + R_H)/3 = [2(R_{d-d} + R_o) + R_H]/3 = [2R_{d-d} + 3R_{\text{obs}}(\text{MoH}_2)]/3$$

$$R_{d-d} = 3[R_{\text{obs}}(\mathbf{1}) - R_{\text{obs}}(\text{MoH}_2)]/2$$

Using the experimental values reported above, $R_{d-d} = 65 \text{ s}^{-1}$.

Applying the method of Halpern, the H–H bond length can be bracketed between 0.8 Å (fast H₂ rotation) and 1.0 Å (slow rotation).¹⁷ In this context, the terms fast and slow are in comparison to molecular tumbling, which is generally very rapid. On the basis of the hindered rotation of dihydrogen

(15) Green, J. C.; Jardine, C. N. *J. Chem. Soc., Dalton Trans.* **1998**, 1057.

(16) Shin, J. H.; Parkin, G. *Chem. Commun.* **1999**, 887.

(17) Desrosiers, P. J.; Cai, L.; Lin, Z.; Richards, R.; Halpern, J. J. *Am. Chem. Soc.* **1991**, 113, 4173. Some confusion about the units employed in the equations describing dipole–dipole relaxation has been recently clarified: Bayse, C. A.; Luck, R. L.; Schelter, E. J. *Inorg. Chem.* **2001**, 40, 3463.

Table 4. Mulliken Atom–Atom Overlap Populations for Ground State Structures

complex	Mo–H _a	Mo–H _b	Mo–H _c	H _a –H _b
1	0.0182	0.0027	0.2464	0.3389
2	0.1813	0.0158	0.1589	0.0966
3	0.1902	0.0758	0.1903	0.0583

Table 5. Population of the σ and σ^* Orbitals of H_a–H_b in the Ground State and C_s Transition State for **1**

	σ	σ^*
1 ground state	1.87	0.25
1 C _s transition state	1.94	0.06

described below, the latter distance is more likely to be correct. A second method based on measurement of $J_{\text{H-D}}$ in the HD ligand is described below which yields a more accurate value for the H₂ bond length.

H–D Coupling in Complex 1. Partial deuteration of the hydride ligands in complex **1** leads to the observation of distinct resonances for **1**, **1-d₁**, and **1-d₂**, in the ¹H NMR spectrum, with the deuterated species exhibiting substantial H–D coupling. The resonances due to **1-d₁** and **1-d₂** are shifted modestly upfield from that due to **1**, by $\Delta\delta = 30$ and 80 ppb, respectively. At 245 K, the H–D coupling in **1-d₁** is 11.9 Hz, while the H–D coupling in **1-d₂** is 9.9 Hz (see Figure 1). These values for $J_{\text{H-D}}$ are indicative of the presence of a dihydrogen ligand. If the deuterium atoms were distributed statistically in a hydride/dihydrogen structure, the two values of $J_{\text{H-D}}$ would be equal and $^1J_{\text{H-D}}$ would be exactly three times this value. The observation of different values of $J_{\text{H-D}}$ in the different isotopomers is characteristic of isotopic perturbation of an equilibrium and a nonstatistical distribution of deuterium. The actual value for $^1J_{\text{H-D}}$ in complex **1** must be between 36 and 30 Hz, which leads to an H–H distance of 0.84–0.94 Å.

In contrast, the $\Delta\delta$ values are essentially independent of temperature, suggesting that the chemical shift differences between the different chemical environments are modest and that much of the observed isotope effect on the chemical shifts can be attributed to *intrinsic* isotope effects. This has been partially verified by low temperature NMR spectra of **1-d₂** (vide infra).

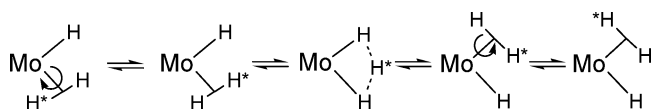
The calculated minimum energy structure for **1** is in good agreement with the experimental findings in that the H₃ system is found to be of the dihydrogen/hydride type. The Mo–H distances correlate with the Mulliken overlap populations given in Table 4.

The calculated H–H distance in the dihydrogen ligand is 0.985 Å (Table 1), slightly outside the range indicated from the H–D coupling constant, though within that given by the relaxation time. Populations of the H₂ σ and σ^* orbitals are given in Table 5. The H_a–H_b distance in the rotated C_s symmetry transition state is 0.828 Å for **1** (see Table 3), showing that back-donation to the H₂ unit has decreased substantially. The occupation of the H₂ σ^* orbitals drops from 0.25 in the ground state to 0.06 in the C_s transition state (Table 5).

Dynamic Behavior of Complex 1. The tungsten complex [Cp₂WH₃]⁺ has static hydride ligands, but the Mo analogue

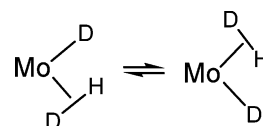
[Cp₂MoH₃]⁺ exhibits rapid exchange of the hydride ligands, leading to a single resonance for the hydride ligands at room temperature.¹¹ Subsequent investigation of the low temperature NMR spectrum of [Cp₂MoH₃]⁺ revealed that the hydride resonances correspond to an AB₂ spin system at low temperature, with $J_{\text{AB}} = 450$ Hz at 153 K.¹² Recent studies on ansa derivatives of the tungsten trihydride reveal that the installation of a bridge between the two cyclopentadienyl rings has a dramatic effect on the hydride dynamics, significantly lowering the activation energy for hydrogen atom exchange. Study of the low temperature ¹H NMR spectra of complexes such as [(η -C₅H₄)₂CMe₂WH₃]⁺ reveals *very* large exchange couplings, with values up to 16000 Hz reported at 200 K.¹³ Smaller, but still significant, exchange couplings were reported for analogues with SiMe₂ and C₂-Me₄ bridges.¹⁸

In the case of complex **1**, we anticipated that the d² configuration would lead to a substantial barrier to H₂ rotation and that the degenerate atom exchange would be slowed sufficiently at low temperature that three distinct hydride resonances could be observed, corresponding to a hydride environment and inner/outer dihydrogen resonances. The diagram below depicts the dynamic process envisaged for this molecule, with the central structure representing a transition state for atom transfer from one side of the molecule to the other.



Surprisingly, ¹H NMR spectra of complex **1** in the hydride region exhibit a single resonance, even when the temperature of observation was lowered to 130 K. This observation may be consistent with a very rapid dynamic process of the type depicted above, in which both atom exchange and dihydrogen ligand rotation are extremely facile. Partially deuterated samples reveal a much more nuanced situation.

Examination of the ¹H NMR spectra of mixtures of **1**, **1-d₁**, and **1-d₂** reveals complex dynamic behavior in the partially deuterated isotopomers. At 140 K, two resonances are observed for complex **1-d₂**. The lower field resonance at –4.28 ppm is a five line pattern due to coupling to two D nuclei, with $J_{\text{H-D}} = 15.6$ Hz. This coupling pattern results from a rapid atom exchange between the two structures depicted below, with the result that the observed $J_{\text{H-D}}$ is equal to $^1J_{\text{H-D}}/2$, consistent with the high temperature observations noted previously, where a value of $^1J_{\text{H-D}} = 30$ –36 Hz was deduced.

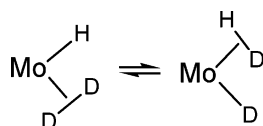


It is important to note that these observations establish that

(18) Conway, S. L. J.; Dijkstra, T.; Doerer, L. H.; Green, M. L. H.; Labella, L.; Stephens, A. H. H. *J. Chem. Soc., Dalton Trans.* **1998**, 2689.

while rotation of the dihydrogen ligand is hindered, degenerate H atom exchange as depicted above is still occurring very rapidly.

The higher field resonance of intensity 2 attributed to $1-d_2$ exhibits no resolvable H–D coupling. The expected H–D coupling in this resonance is $^1J_{\text{H-D}}/2$, which would be ca. 15.6 Hz. This outcome is readily explicable in terms of the atom exchange process depicted below. The single hydrogen atom in $1-d_2$ interacts with a single deuteron, but only one of the two structures depicted below leads to a significant coupling.

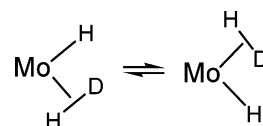


The line width of this resonance at 140 K is ca. 15 Hz. Our failure to observe this coupling is attributed to the occurrence of a large DD exchange coupling, which has precedent in the observations of Otero and co-workers¹⁹ for $[(\eta\text{-C}_5\text{H}_4\text{-SiMe}_3)_2\text{Nb}(\text{CNR})(\text{H}_2)]^+$ and Chaudret and co-workers²⁰ for $[(\eta\text{-C}_5\text{H}_4\text{SiMe}_3)_2\text{Nb}(\text{PR}_3)(\text{H}_2)]^+$.

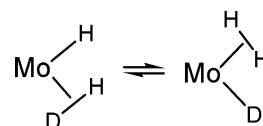
Upon raising the temperature of observation, the resonances attributed to $1-d_2$ broaden and coalesce at ca. 180 K. Computed line shapes for spectra collected in the temperature range 140–180 K were matched to experimental data to extract the rate of hydrogen ligand rotation. An Eyring plot of this data gives $\Delta H^\ddagger = 7.3$ kcal/mol, $\Delta S^\ddagger = -0.3$ cal/mol deg, and $\Delta G^\ddagger_{150} = 7.4$ kcal/mol. This barrier for hydrogen rotation is comparable to previously reported observations in d^2 Ta and Nb dihydrogen complexes.¹⁰ Frequency calculations on **1** were used to determine ΔG^\ddagger_{150} for **1** for H_aH_b exchange at 150 K giving a value of 10 kcal/mol (see Supporting Information). In this case, with the H–H bond formed in the ground state, zero point energy differences between the ground and the transition state made little difference to the estimated energy barrier. The calculated solvent effects at 298 K using the COSMO solvent model²¹ indicate that the activation energy may be reduced by a further 1.5 kcal/mol. Thus the experimental and calculated values are in reasonable agreement. A thermodynamic analysis for all three systems is included in the Supporting Information.

Very different NMR signals are observed at 140 K for the resonances attributed to $1-d_1$. Two signals are again observed, with a broad singlet at -5.35 ppm (2H) and a 1:1:1 triplet ($J_{\text{H-D}} = 15.6$ Hz) at -6.55 ppm (1H) (see Figure 2). The upfield resonance is attributed to a situation where H atoms are interacting with a single deuteron as shown below. As noted above, this leads to an observed H–D coupling equal to $^1J_{\text{H-D}}/2$.

The broad singlet at lower field is assigned to the form of $1-d_1$ where the single deuteron is in the “outside” chemical



environment and the two H atoms are adjacent, as depicted below. Since the anticipated H–D coupling is again $^1J_{\text{H-D}}/2$, this modest coupling is not resolved. Given that H_2 rotation was found to be hindered in $1-d_1$, it is reasonable to anticipate that *two* distinct chemical environments for H atoms would result from the situation below, corresponding to “inside” and “outside” locations for the H atom.



The observation of a single hydride resonance at low temperature for the molecule depicted above suggests that some other process is operating to render the two chemical environments equivalent. We suggest that this is the result of a large exchange coupling between the two H atoms of the bound dihydrogen moiety. In an AB spin system, large values of J_{AB} can lead to a single resonance if J_{AB} is ca. $50\Delta\delta$. Our data do not permit an evaluation of the chemical shift difference between the two ends of the bound dihydrogen ligand. Essentially the same situation was reported by Chaudret and co-workers¹⁰ for $[\text{Cp}_2\text{Ta}(\text{CO})(\text{H}_2)]^+$, where hindered hydrogen rotation was observed for bound HD, but a single resonance was seen for bound H_2 . This was attributed to the operation of a very large exchange coupling in the bound dihydrogen ligand. Chaudret and co-workers were able to directly observe the chemical shift difference between the two ends of the bound H–D, which was reported to be 0.64 ppm. Assuming a similar chemical shift difference in complex **1**, we estimate an H–H exchange coupling in the bound dihydrogen ligand in **1** of *at least* 24000 Hz, based on the observation of a single resonance for this AB spin system even at 750 MHz. We note that this value is critically dependent on the *assumed* chemical shift difference, and would be correspondingly reduced if $\Delta\delta$ in complex **1** is smaller than observed in the complex studied by Chaudret and co-workers.

Frequency calculations on **1** were used to estimate ΔG^\ddagger_{150} for **1** for H_aH_c exchange at 150 K giving a value of 0.69 kcal/mol (see Supporting Information). This very low barrier would indicate extremely large exchange coupling, as is found experimentally.

These considerations also allow us to understand the observation of a single resonance for complex **1** at all accessible temperatures when no deuterium is incorporated in the hydride ligands. Rapid atom exchange combined with large exchange coupling when two H atoms are adjacent leads to the observed single resonance.

Isotopic Perturbation Effects. As previously reported for an iridium hydride/dihydrogen complex, the observed chemical shifts and $J_{\text{H-D}}$ coupling data can in principle be analyzed quantitatively to calculate the limiting chemical shifts of the

- (19) Antinolo, A.; Carillo-Hermosilla, F.; Fajardo, M.; Garcia-Yuste, S.; Otero, A.; Camanyes, S.; Maseras, F.; Moreno, M.; Lledos, A.; Lluch, J. M. *J. Am. Chem. Soc.* **1997**, *119*, 6107.
 (20) Jalon, F. A.; Otero, A.; Manzano, B. R.; Villasenor, E.; Chaudret, B. *J. Am. Chem. Soc.* **1997**, *119*, 10123.
 (21) Pye, C. C.; Ziegler, T. *Theor. Chem. Acc.* **1999**, *101*, 396.

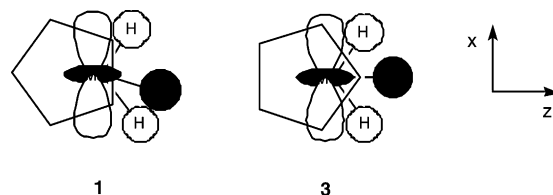
dihydrogen ligand (δ_{H_2}) and the terminal hydride ligand (δ_H), $^1J_{H-D}$ for the HD ligand, and the energy difference which arises from deuterium substitution at the different sites.⁷ In the case of complex **1**, this analysis is complicated by the relatively small isotope effects observed upon deuteration, which are attributed in part to the intrinsic isotope effects on the hydride chemical shifts expected to result from partial deuteration. A further complication arises from the rapid atom exchange process described above, which leads to averaging of chemical shifts even at low temperature.

A value of $^1J_{H-D}$ can be extracted from the low temperature 1H NMR spectra of the isotopomers of complex **1**. In **1**- d_2 , the low field resonance is a five line pattern where the observed H–D coupling is equal to $^1J_{H-D}/2$. Similarly, complex **1**- d_2 exhibits in the upfield resonance a three line pattern with coupling equal to $^1J_{H-D}/2$. Both of these couplings are observed to be 15.6 Hz, so $^1J_{H-D} = 31$ Hz. The averaged J_{H-D} observed for **1**- d_2 at high temperature is 9.9 Hz, which would give a value for $^1J_{H-D} = 29.7$ Hz if deuterium distribution is statistical. We can thus conclude that, in this isotopomer, the distribution of deuterium among the different chemical environments is only slightly perturbed from a statistical distribution, with a very slight preference for D to concentrate in the dihydrogen ligand.

The average value of J_{H-D} for **1**- d_1 observed at high temperature is 11.9 Hz, which suggests a greater perturbation from a statistical deuterium distribution in this isotopomer, with D concentrated significantly in the dihydrogen ligand. These observations are qualitatively similar to those previously reported for a rhodium dihydrogen/hydride complex, where deuterium was also concentrated in the dihydrogen ligand.²² In contrast, an iridium dihydrogen/hydride complex exhibits concentration of deuterium in the hydride, rather than the dihydrogen ligand.⁷ Since second row metals generally form weaker M–H bonds than third row metals and D tends to concentrate in the stronger bond, it is reasonable that complex **1** exhibits concentration of D in the dihydrogen ligand. Frequency calculations at 298 K on **1**- d_1 give relative free energies for the three isotopomers of 0, 0.071, and 0.071 kcal/mol for the D in H_a , H_b , and H_c sites, respectively, indicating a small preference for deuterium to accumulate in the H_2 ligand.

Electronic Structure Considerations. The change from a H_2/H structure to a trihydride structure can be formally represented as an oxidation of the metal, in the present case from Mo^{IV} to Mo^{VI} . The difference in the structure of **1** and its W analogue, which has a trihydride structure, is readily understood in these terms as W is easier to oxidize than Mo. The role of ansa bridges in affecting the ease of oxidation at the metal is also well documented.^{23–25}

In a d^2 bent metallocene the two electrons occupy a $d(x^2)$ orbital pointing across the metallocene plane.²⁶ This orbital has the capacity to back-bond to the cyclopentadienyl rings. The degree of back-bonding is very sensitive to the ring orientation and is maximized with conformation **B**, and minimized with conformation **A**.²¹ The $d(x^2)$ orbital also provides a nodal match with the $1s_a - 1s_b + 1s_c$ linear combination of the trihydride 1s orbitals. This antibonding combination of the three H 1s orbitals lies higher in energy than the metal $d(x^2)$ orbital and competes for back-donation with the cyclopentadienyl rings. The more the rings stabilize the $d(x^2)$ orbital, the less it is available to bond to the three hydrogens.



Thus the ground-state structure of **3** (Mo^{VI}) has ring conformation **A** whereas the transition state for H_aH_b exchange which has the rotated H_2 unit (Mo^{IV}) has ring conformation **B**. In the rotated transition state there is no back-bonding to the H ligands from the $d(x^2)$ orbital; they lie in its nodal plane; thus it is stabilized by the rings adopting conformation **B**. Compound **1** with the ansa-C bridge is sufficiently strained that the rings are fixed in conformation **B**; this cuts down on back-donation to the hydrogen atoms and favors the IV oxidation state for Mo with the consequence that the ground state is of the H_2/H type and the barrier to H_2 rotation is modest. For **2**, the Si bridge is less strained and both ring conformations are possible, as is found for **3**.

Contour plots for the HOMOs of **1** and **3**, both in their ground states and their C_s transition states, are shown in Figure 3. In the ground states the greater localization of the HOMO of **1** on the metal is evident. For both C_s transition states both the rotated H_2 unit and the hydride lie in the nodal plane of the HOMO, which is consequently localized on the metal.

Conclusion

We find that $[(\eta-C_5H_4)_2CMe_2MoH(H_2)]^+$ is the first example of a dihydrogen/hydride complex with a d^2 configuration. DFT calculations are consistent with the experimentally determined structure. The dihydrogen ligand exhibits hindered rotation as revealed by low temperature NMR spectroscopy of partially deuterated samples. The measured barrier to rotation is in good agreement with the results of DFT calculations. While hydrogen rotation has a significant barrier, H atom transfer between the dihydrogen moiety and the adjacent hydride remains extremely rapid at all accessible temperatures. Significant differences in the low temperature NMR spectra of the isotopomers of **1** are attributed to the

(22) Taw, F. L.; Mellows, H.; White, P. S.; Hollander, F. J.; Bergman, R. G.; Brookhart, M.; Heinekey, D. M. *J. Am. Chem. Soc.* **2002**, *124*, 5100.

(23) Green, J. C.; Scottow, A. *New J. Chem.* **1999**, *23*, 651.

(24) Zachmanoglou, C. E.; Docrat, A.; Bridgewater, B. M.; Parkin, G.; Brandow, G.; Bercaw, J. E.; Jardine, C. N.; Lyall, M.; Green, J. C.; Keister, J. B. *J. Am. Chem. Soc.* **2002**, *124*, 9525.

(25) Ackerman, L. J.; Green, M. L. H.; Green, J. C.; Bercaw, J. E. *Organometallics* **2003**, *22*, 188.

(26) Green, J. C. *Chem. Soc. Rev.* **1998**, *27*, 263.

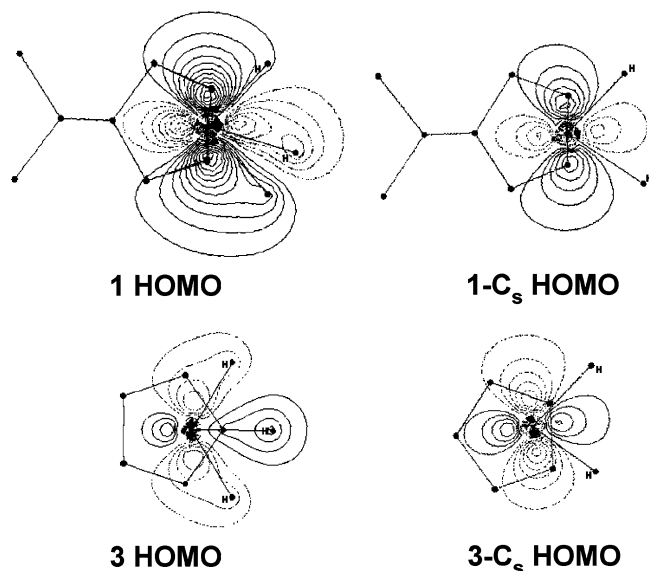


Figure 3. Contour plots for the HOMOs of **1** and **3**. Left: ground state. Right: C_s transition states.

occurrence of exchange coupling, which is important when two H or D atoms are adjacent, leading to deceptively simple spectra. We note that related trihydride complexes such as $[(\eta\text{-C}_5\text{H}_5)_2\text{MoH}_3]^+$ have higher barriers to hydrogen atom permutation. In light of the current observations on complex **1**, the intermediacy of a dihydrogen/hydride species in the hydrogen atom permutation process seems plausible for metallocene trihydride complexes in general.

We are continuing to investigate the structure and dynamics of dihydrogen/hydride complexes with d^2 configurations. Such complexes are structurally very close to the long sought trihydrogen complexes.

Experimental Section

General Methods. Unless stated otherwise, all manipulations were carried out under argon using Schlenk or drybox techniques. $[\text{H}(\text{Et}_2\text{O})_2][\text{BARf}_4]$ and $(\eta\text{-C}_5\text{H}_4)_2\text{CMe}_2\text{MoH}_2$ were synthesized as described in the literature. Deuterated solvents (Cambridge Isotope Laboratories) were dried over CaH_2 . Deuterated Freon 21 (CDFCl_2), 22 (CDF_2Cl), and 23 (CDF_3) were prepared by the method of Anet²⁷ and stored in a glass bomb over calcium hydride. $(\text{CF}_3\text{SO}_2)_2\text{CH}_2$ was the generous gift of Dr. Allen Siedle (3M). The deuterated acid $(\text{CF}_3\text{SO}_2)_2\text{CD}_2$ was made by exchanging $(\text{CF}_3\text{SO}_2)_2\text{CH}_2$ with CH_3OD followed by sublimation. CF_3COOD was purchased from Aldrich and used as received. Hydrogen gas was purchased from Airgas and passed through a column of activated molecular sieves prior to use. D_2 gas was purchased from Cambridge Isotope Laboratories. NMR spectra were recorded on Bruker AV 500, DRX 499, and DMX 750 spectrometers. Proton NMR spectra were referenced to the solvent resonance with chemical shifts reported relative to TMS. The NMR studies were carried out in high quality 5 mm NMR tubes. The workup of spectra used for precise measuring of coupling constants used zero filling to 128K data points prior to Fourier transform.

$[(\eta\text{-C}_5\text{H}_4)_2\text{CMe}_2\text{Mo}(\text{H})_2\text{H}]\text{B}(\text{ArF})_4$. A screwcap NMR tube (J-Young) was charged with 5 mg of $(\eta\text{-C}_5\text{H}_4)_2\text{CMe}_2\text{MoH}_2$ (0.018 mmol) and 20 mg of $[3,5\text{-(CF}_3)_2\text{C}_6\text{H}_3]_4\text{B}(\text{OEt})_2$ (0.019 mmol).

(27) Siegel, J. S.; Anet, F. A. *J. Org. Chem.* **1988**, *53*, 2629.

CD_2Cl_2 (1–2 mL) was condensed into the NMR tube, which was then sealed at 200 K. ^1H NMR, δ (CD_2Cl_2 , 750 MHz, 245 K): 5.55, 5.17 (s, 8H, C_5H_4), 1.24 (s, 6 H, CMe_2), -5.59 (s, 3 H $\text{Mo}(\text{H}_2)\text{H}$).

1- d_1 and - d_2 . Deuterium incorporation was achieved by protonation of a methylene chloride (or Freon) solution of $(\eta\text{-C}_5\text{H}_4)_2\text{CMe}_2\text{MoH}_2$ with 1 to 20 equivalents of deuterated acid CF_3COOD or $\text{D}_2\text{C}(\text{SO}_2\text{CF}_3)_2$. ^1H NMR, δ (CD_2Cl_2 , 750 MHz, 245 K): -5.59 (s), -5.61 (t), -5.68 (quint), ($\text{MoH}_3\text{-}d_0$, $-d_1$, $-d_2$).

Computational Methods. Calculations were performed using ADF v2002.03^{28–30} using the Vosko, Wilke, and Nusair local functional³¹ with the Becke 88^{32,33} and Perdew 86³⁴ nonlocal exchange and correlation gradient corrections. The basis sets used were uncontracted triple- ζ Slater-type orbitals (STOs). Hydrogen, deuterium, and carbon were given extra polarization functions (2p on H and 3d on C). The cores of atoms were frozen, C up to the 1s level, Si up to the 2p level, and Mo up to the 3d level. Scalar ZORA relativistic corrections^{35–38} were used. Stationary points were verified as either a ground state or transition state by full frequency calculations^{39,40} with either zero or one imaginary eigenvector in the Hessian. Transition states were verified with IRC calculations.^{41,42} Cartesian coordinates for all stationary points are given in the Supporting Information. During a linear transit, one or more internal variables (internuclear distance or angle) were fixed to successive values as a reaction coordinate and all other variables were optimized. The calculation of solvent effects used the COSMO model implemented into ADF by Pye and Ziegler.²⁰ The calculation was done on the solvent excluding surface using the default radii for the program, using a dielectric constant of 9.08 corresponding to dichloromethane. Thermodynamic activation energies were calculated using the formula

$$\Delta G^\ddagger_{\text{T}} = G_{\text{T}}(\text{products}) - G_{\text{T}}(\text{reactants})$$

$$G_{\text{T}} = E_{\text{SCF}} + E_{\text{ZPE}} + E_{\text{int}}(T) - TS(T)$$

They therefore represent gas phase free energies. Solvent corrections

- (28) Baerends, E. J.; Autschbach, J. A.; Berces, A.; Bo, C.; Boerringer, P. M.; Cavallo, L.; Chong, D. P.; Deng, L.; Dickson, R. M.; Ellis, D. E.; Fan, L.; Fischer, T. H.; Fonseca-Guerra, C.; van Gisbergen, S. J.; Groeneveld, J. A.; Gritsenko, O. V.; Grüning, M.; Harris, F. E.; van den Hoek, P.; Jacobsen, H.; van Kessel, G.; Kootstra, F.; van Lenthe, E.; Osinga, V. P.; Patchkovskii, S.; Philipsen, P. H. T.; Post, D.; Pye, C. C.; Ravenek, W.; Ros, P.; Schipper, P. R. T.; Schreckenbach, G.; Snijders, J. G.; Sola, M.; Swart, M.; Swerhone, D.; te Velde, G.; Vernooijis, P.; Versluis, L.; Visser, O.; van Wezenbeek, E.; Wiesenekker, G.; Wolff, S. K.; Woo, T. K.; Ziegler, T. Amsterdam Density Functional, 2nd ed.; Scientific Computing & Modelling NV: Vrije Universiteit, Amsterdam, 2002.
- (29) te Velde, G.; Bickelhaupt, F. M.; Baerends, E. J.; Fonseca Guerra, C.; Van Gisbergen, S. J. A.; Snijders, J. G.; Ziegler, T. *J. Comput. Chem.* **2001**, *22*, 931.
- (30) Guerra, C. F.; Snijders, J. G.; te Velde, G.; Baerends, E. J. *Theor. Chem. Acc.* **1998**, *99*, 391.
- (31) Vosko, S. H.; Wilk, L.; Nusair, M. *Can. J. Phys.* **1980**, *58*, 1200.
- (32) Becke, A. D. *Phys. Rev. A* **1988**, *38*, 3098.
- (33) Becke, A. D. *J. Chem. Phys.* **1988**, *88*, 1053.
- (34) Perdew, J. P. *Phys. Rev. B* **1986**, *33*, 8800.
- (35) van Lenthe, E.; Baerends, E. J.; Snijders, J. G. *J. Chem. Phys.* **1993**, *99*, 4597.
- (36) van Lenthe, E.; Baerends, E. J.; Snijders, J. G. *J. Chem. Phys.* **1994**, *101*, 9783.
- (37) van Lenthe, E.; Snijders, J. G.; Baerends, E. J. *J. Chem. Phys.* **1996**, *105*, 6505.
- (38) van Lenthe, E.; van Leeuwen, R.; Baerends, E. J.; Snijders, J. G. *Int. J. Quantum Chem.* **1996**, *57*, 281.
- (39) Fan, L.; Ziegler, T. *J. Chem. Phys.* **1992**, *96*, 9005.
- (40) Fan, L.; Ziegler, T. *J. Phys. Chem.* **1992**, *96*, 6937.
- (41) Deng, L.; Ziegler, T.; Fan, L. *J. Chem. Phys.* **1993**, *99*, 3823.
- (42) Deng, L.; Ziegler, T. *J. Quantum. Chem.* **1994**, *52*, 731.

were not included as their calculation requires temperature dependent variables which are only reliably available for 298.15 K. H_a and H_b form the rotating H₂ units.

Acknowledgment. The research at the University of Washington was supported by the National Science Foundation. Acquisition of the 750 MHz NMR spectrometer was supported by the National Science Foundation and the Murdoch Charitable Trust. Calculations were performed

using the facilities at the Oxford Supercomputer Center. We thank EPSRC for studentship support (B.J.H. and S.L.J.C.).

Supporting Information Available: Computational details for **1–3**, including Cartesian coordinates for all stationary points. Variable temperature ¹H NMR spectra of **1**. This material is available free of charge via the Internet at <http://pubs.acs.org>.

IC0496875